(TPP)(1-MeIm)$_2$] structure, are most consistent with the bis-(imidazole)iron(II) complexes having the same well-developed axial ligand orientation preferences as all other metalloporphyrin species.

Scheidt and Chipman[43] have attempted to define the fundamental electronic reasons for these apparent ligand orientation preferences. They carried out iterative extended Hückel calculations on a number of imidazole-ligated metalloporphyrins as a function of axial ligand orientation angle. From these rotational calculations they suggested that imidazole ligand π donation to metal pπ and dπ orbitals leads to the preference for the small ϕ ligand orientations. In the iron(III) systems, in which there are unequally filled metal dπ orbitals, ligand pπ to metal dπ bonding favors the parallel ligand relative orientation. This bonding effect, however, does not explain the parallel relative orientation preference of other bis(imidazole) metalloporphyrin derivatives. The present iron(II) results do not shed further light on this issue. We may note, however, the fact that bis(hindered imidazole)iron(II) complexes cannot be prepared (except perhaps at very low temperatures[45]) is consistent with a strong tendency for parallel ligand

orientation. Walker et al.[4] have discussed the possible effects of varying axial ligand orientation on the redox potentials of the Fe$^{II/III}$ couple of cytochromes *b*. They suggested that a perpendicular orientation of the two axial imidazole ligands could yield a more positive redox potential. (However, the effect could yield no more than 50 mV.) The apparently well-developed parallel axial ligand preference in bis(imidazole)iron(II) species demonstrated in this paper is consistent with this possible orientation effect on the redox potential.

Supplementary Material Available: Table IS, listing complete crystal data and intensity collection parameters, Tables IIS and IIIS, giving anisotropic thermal parameters and fixed hydrogen atom positions for [Fe(TPP)(1-VinIm)$_2$], Tables IVS and VS, listing anisotropic thermal parameters and fixed hydrogen atom positions for [Fe(TPP)(1-BzlIm)$_2$], and Tables VIS and VIIS, giving bond distances and angles for [Fe-(TPP)(1-MeIm)$_2$] (9 pages); listings (×10) of observed and calculated structure amplitudes for [Fe(TPP)(1-VinIm)$_2$] and [Fe(TPP)(1-BzlIm)$_2$] (30 pages). Ordering information is given on any current masthead page.

(45) Wang, C.-M.; Brinigar, W. S. *Biochemistry* **1979**, *18*, 4960–4977.

Contribution from the Department of Chemistry, Boston College, Chestnut Hill, Massachusetts 02167-3809

Synthesis and Electrochemistry of Pterins Coordinated to Tetraammineruthenium(II)

Angel Abelleira, Roy D. Galang, and Michael J. Clarke*

Compounds of the general type *cis*-[L(NH$_3$)$_4$Ru]Br$_2$, in which the Ru(II) is coordinated between the N5 and O4 sites, have been synthesized, where L = lumazine, 1,3-dimethyllumazine, 3-methylpterin, 8-methylpterin, and 3,6,7-trimethylpterin. These complexes have been characterized as to their electrochemistry and electronic and fluorescence spectra. Voltammetry and controlled-potential coulometry show that coordinated pterins methylated at N3 undergo a 1e redox process, which is reversible in DMF on the CV time scale. Intense retrodative bonding with Ru(II) raises the potential for the Ru(III,II) couple to the range 560–720 mV and alters the site of protonation to N8.

Owing to the close association of metal ions and pterin coenzymes in many biological redox processes, we have prepared a series of pterin complexes, using Ru(II) to attain a stable metal–pterin bond, to investigate the spectroscopic and electrochemical effects of pterin coordination and show that single-electron transfer is possible for some pteridine ligands when coordinated at the N5 position. Pterin cofactors (derivatives of 2-amino-4(3*H*)-pteridinone) undergo complex redox processes (see Figure 1) and are essential to the function of a number of important metal-containing redox enzymes.[1,2] Examples are (1) the iron-requiring phenylalanine, tyrosine, and tryptophan monooxygenases (2) formate dehydrogenase, which contains W, Se, and Fe,[3] and (3) the molybdenum cofactor (Mo–co), which involves metal coordination of a pterin side chain and occurs in at least ten different enzymes, including nitrate reductase, sulfite oxidase, and xanthine oxidase.[4–7] There is also some evidence that pterins

may be involved in photobiological processes.[8]

Phenylalanine 4-monooxygenase requires a 6-substituted tetrahydrobiopterin, which is in close association with an iron center,[9,10] to catalyze the conversion of phenylalanine to tyrosine. This product undergoes a subsequent conversion by tyrosine 3-monooxygenase to dopa (3,4-dihydroxyphenylalanine), a precursor for the neurotransmitters epinephrine and norepinephrine.[11] In the genetic absence of this enzyme (phenylketonuria), phenylpyruvic acid accumulates in the blood to impair brain development. The quinonoid dihydropterin produced in pterin enzymatic processes is reduced by dihydropterin reductase in the presence of NADPH or NADH back to the tetrahydropterin.[12] The phenylalanine hydroxylase from *Chromobacterium violaceum* appears to involve a type 2 copper center, which may be coordinated to a reduced pterin ring.[13]

The coordination chemistry of pteridines has received relatively little attention. Albert originally investigated complexes of 8-

(1) Coughlan, M. *Molybdenum and Molybdenum Containing Enzymes*; Pergamon Press: New York, 1980.
(2) *Molybdenum Enzymes*; Spiro, T. G., Ed.; Wiley-Interscience: New York, 1985.
(3) Yamamoto, I.; Saiki, T.; Liu, S.-M.; Ljungdahl, L. G. *J. Biol. Chem.* **1983**, *258*, 1826.
(4) Johnson, J. L.; Hainline, B. E.; Rajagopalan, K. V. *J. Biol. Chem.* **1980**, *255*, 1783.
(5) Johnson, J. L.; Rajagopalan, K. V. *Proc. Natl. Acad. Sci. U.S.A.* **1982**, *79*, 6856.
(6) Davis, M. D.; Olson, J. S.; Palmer, G. *J. Biol. Chem.* **1982**, *257*, 14730.
(7) Harlan, E. W.; Berg, J. M.; Holm, R. H. *J. Am. Chem. Soc.* **1986**, *108*, 6992–7000 and references therein.

(8) Chanhidi, C.; Aubailly, M.; Momzikoff, A.; Bazin, M.; Santus, R. *Photochem. Photobiol.* **1981**, *33*, 641.
(9) Dix, T. A.; Bollag, G. E.; Domanico, P. L.; Benkovic, S. J. *Biochemistry* **1985**, *24*, 2955.
(10) Wallick, D. E.; Bloom, L. M.; Gaffney, B. J.; Benkovic, S. J. *Biochemistry* **1984**, *23*, 1295.
(11) (a) Kaufman, S. *J. Biol. Chem.* **1957**, *226*, 511. (b) Kaufman, S. *J. Biol. Chem.* **1958**, *230*, 931. (c) Kaufman, S. *Proc. Natl. Acad. Sci. U.S.A.* **1963**, *50*, 1085. (d) Kaufman, S. *J. Biol. Chem.* **1964**, *239*, 332.
(12) Crane, J. E.; Hall, E. S.; Kaufman, S. *J. Biol. Chem.* **1972**, *247*, 6082.
(13) Pember, S. O.; Benkovic, S. J.; Villagranca, J. J.; Pasenkiewicz-Gierula, M.; Antholine, W. E. *Biochemistry* **1987**, *26*, 4477–83.
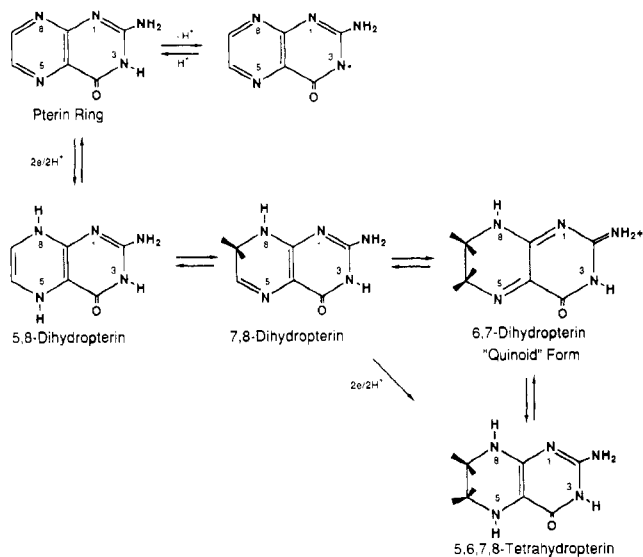
Figure 1. Redox and proton equilibria for pterin (2-amino-4-pteridinol).

hydroxyquinoline and several pterins,[14] which, while coordinating metal cations through an oxygen peri to a tertiary heterocyclic nitrogen, exhibited substantially lower affinities than the 8-hydroxyquinoline. Nevertheless, the pteridines exhibited higher affinities than glycine, proline, and many other common amino acids for Fe(II), Ni(II), Co(II), Cd(II), and Mn(II) at physiological pH.[15] Goodgame and Schmidt described a series of O4–N5 chelated complexes of lumazine with divalent metal ions, in which complexes made in aqueous solution at pH 6.3 were reported to contain anionic lumazine, while those from organic solvents involved the neutral ligand.[16] A model molybdenum-pterin complex contains a *syn*-$[Mo_2O_5]^{2+}$ unit chelated by O3 and N5 of one xanthopterinate and is bridged to the O4 of a second xanthopterinate.[17] In this complex there is essentially complete quenching of the fluorescence of the ligand, indicating that metal ion coordination may account for the disappearance of pterin fluorescence in biological systems. Unfortunately, no electrochemical studies were reported for this model.

Studies of enzymatic oxidations at C7 of lumazine, by xanthine oxidase, suggest that the carbonyl at C4 is involved, presumably as a coordination site.[18] Anaerobic addition of lumazine to xanthine oxidase leads to the formation of a species absorbing at long wavelength (λ_{max} = 650 nm).[19] A similar species is obtained when lumazine or 2,4,7-trihydroxypteridine is added to the dithionite-reduced enzyme and is thought to arise from a charge-transfer complex between Mo(IV) and the pteridine.

In an electrochemical study of Fe(II) with tetrahydropterin at pH 3.2,[20] Fe(III) appeared to oxidize tetrahydropterin and 7,8-dihydropterin. Oxidation of tetrahydropterin initially produced a compound similar to a quinonoid dihydropterin,[21] which converted relatively slowly to 7,8-dihydropterin via a first-order process that increased with pH. Some evidence suggested that 7,8-dihydropterin is probably not oxidized by Fe(III) but may undergo further reaction with the quinonoid dihydropterin to give oxidized pterin and tetrahydropterin, which could then be oxidized by Fe(III).

Folic acid is oxidatively cleaved at the side chain by $[(bpy)Cu]^{2+}$ and the corresponding *o*-phenanthroline complex at pH > to give a complex with pterin-6-carboxylate.[22] The crystal structure of

$[(bpy)(pterin-6-carboxylate)(H_2O)Cu]$ shows a dianionic pterin coordinated at N5 with weaker bonding through the carboxylate and C4 oxygens in the apical positions. The ESR spectrum lent support to the conclusion that the Cu(II) site in *C. violaceum* phenylalanine hydroxylase consists of two imidazoles, a displaceable water, and possibly a pterin cofactor bound through the ring nitrogen.[13,22]

The electrochemistry of the structurally closely related flavins is strongly influenced by the coordination of Lewis acids at the N1 or N5 positions. Coordination of a proton, alkyl group, or a metal ion at N5 usually results in single-electron transfer by the flavin.[23] On the other hand, coordination at N1 favors 2e transfer.[24] In contrast, pterins[25] almost invariably undergo $2H^+/2e$ processes[26] on all but the shortest of time sscales. Single-electron-transfer kinetics have only been observed by extremely rapid-pulse radiolytic methods,[27] and thermodynamic resolution of these processes has been suggested only in an electrochemical study of 8-methylpterin.[28]

Abbreviations: Lum, lumazine (2,4(1*H*,3*H*)-pteridinedione); 1,3-Me_2Lum, 1,3-dimethyllumazine (1,3-dimethyl-2,4-(1*H*,3*H*)-pteridinedione); 3-MeP, 3-methylpterin (2-amino-3,4-dihydro-3-methyl-4-oxopteridine); 8-MeP, 8-methylpterin (2-amino-4,8-dihydro-8-methyl-4-oxopteridine); 3,6,7-Me_3P, 3,6,7-trimethylpterin (2-amino-3,4-dihydro-3,6,7-trimethyl-4-oxopteridine); Rib, riboflavin.

Lumazine   Pterin Ring
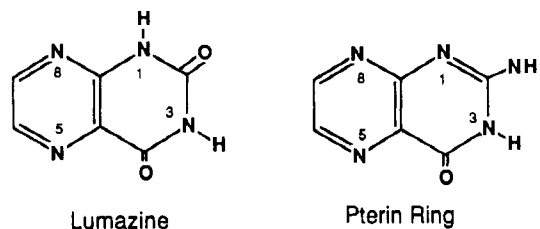
Experimental Section

Synthesis. The ligands 3-MeP,[29,30] 3,6,7-Me_3P, 8-MeP,[31,32] and 1,3-Me_2Lum[33] were synthesized by literature methods. 3-MeLum was isolated from the preparations of 1,3-dimethyllumazine. Lumazine (Aldrich) was used without further purification. $[Cl(NH_3)_5Ru]Cl_2$,[34,35] *cis*-$[Cl_2(NH_3)_4Ru]Cl$,[36] and *cis*-$[(H_2O)_2(NH_3)_4Ru](CF_3SO_3)_3$ were prepared by literature syntheses.[37]

$[Lum(NH_3)_4Ru]Br_2$ was made by dissolving 100 mg of *cis*-$[(H_2O)_2-(NH_3)_4Ru](F_3CSO_3)_2$ or *cis*-$[Cl_2(NH_3)_4Ru]Cl$ in 3 mL of water (pH 3–3.5) and reducing to Ru(II) with amalgamated zinc for 30 min while argon was bubbled through the solution. Meanwhile, a 1.5-fold excess of lumazine was dissolved in about 3.5 mL of water while this mixture was heated on a steam bath and simultaneously deaerated with argon for 30 min. After complete dissolution, the pH of the solution was lowered to 3–3.5 with dilute trifluoromethanesulfonic acid. When both solutions had been deaerated, the ruthenium solution was injected into the lumazine solution, and the color immediately changed from light yellow to dark blue. After continuously being purged with argon for 1 hour, the

(14) Albert, A. *Biochem. J.* **1950**, *47*, 531; **1953**, *54*, 646.
(15) Albert, A. *Biochem. J.* **1950**, *47*, ix.
(16) Goodgame, M.; Schmidt, A. *Inorg. Chim. Acta* **1979**, *36*, 151.
(17) Burgmayer, S. J. N.; Steifel, E. I. *J. Am. Chem. Soc.* **1986**, *108*, 8310–11.
(18) Bunting, J. W.; Gunasekara, A. *Biochim. Biophys. Acta* **1982**, *704*, 444.
(19) Davis, M. D.; Olson, J. S.; Palmer, G. *J. Biol. Chem.* **1982**, *257*, 14730.
(20) Vonderschmitt, D. J.; Scrimgeour, K. G. *Biochem. Biophys. Res. Commun.* **1967**, *28*, 302.
(21) Kaufman, S. *J. Biol. Chem.* **1959**, *234*, 2677.

(22) Kohzuma, T.; Masuda, H.; Yamauchi, O. *J. Am. Chem. Soc.* **1989**, *111*, 3431–2.
(23) Clarke, M. J.; Dowling, M. G. *Inorg. Chem.* **1981**, *20*, 3506–3514.
(24) Dowling, M. G.; Clarke, M. J. *Inorg. Chim. Acta* **1983**, *78*, 153–160 and references therein.
(25) 2-Amino-4(3*H*)-pteridinones.
(26) (a) Kaufman, S. *J. Biol. Chem.* **1964**, *239*, 332. (b) Vonderschmitt, D. J.; Scrimgeour, K. B. *Biochem. Biophys. Res. Commun.* **1967**, *28*, 302. (c) Kwee, S.; Lund, H. *Biochim. Biophys. Acta* **1973**, *298*, 285.
(27) (a) Moorthy, P. N.; Hayon, E. *J. Org. Chem.* **1976**, *41*, 1607–13. (b) Moorthy, P. N.; Hayon, E. *J. Phys. Chem.* **1975**, *79*, 1059–62.
(28) Braun, H.; Pfleiderer, W. *Liebigs Ann. Chem.* **1973**, 1099.
(29) Pfleiderer, W.; Liedek, E.; Lohrmann, R.; Rukwied, M. *Chem. Ber.* **1960**, *93*, 2015.
(30) Pfleiderer, W. *Chem. Ber.* **1957**, *90*, 2272.
(31) Curran, W. V.; Angier, R. B. *J. Am. Chem. Soc.* **1958**, *80*, 6095.
(32) Brown, D. J.; Jacobsen, N. W. *J. Chem. Soc.* **1961**, 4413.
(33) Mager, H. I. X.; Berends, W. *Recl. Trav. Chim. Pays-Bas* **1972**, *91*, 1137.
(34) Vogt, L. H.; Katz, J. L.; Wiberly, S. E. *Inorg. Chem.* **1965**, *4*, 1157.
(35) Allen, A. D.; Bottomley, F.; Harris, R. O.; Reinslau, V. P.; Senoff, C. V. *J. Am. Chem. Soc.* **1967**, *89*, 5595.
(36) Pell, S. D.; Sherban, M. M.; Tramontano, V.; Clarke, M. J. *Inorg. Synth.*, in press.
(37) Diamond, S. E. Ph.D. Thesis, Stanford University, 1975.

solution was bubbled with oxygen for 15 min to reoxidize any unreacted ruthenium.

Purification was carried out by filtering and passing the reaction mixture through a 15 × 2.5 cm Sephadex SP C-25 column. The column was first eluted with water to remove anionic and neutral molecules, followed by elution with 0.05 M HBr. The desired band eluted with 0.15 M HBr. This solution was rapidly rotary-evaporated to dryness, and the complex was redissolved in water and rotary-evaporated to dryness again. The remaining solid was taken up in a minimum amount of water, and 2-propanol was added to induce precipitation as a blue amorphous powder. Slower precipitation, which usually gave crystalline-appearing products, resulted in partial decomposition, as indicated by HPLC. The powder was suction filtered out of the mixture, washed with 2-propanol and ethyl ether, and then dried under vacuum. HPLC: $k' = 0.53$. Anal. Calcd for [$H_{16}C_6N_8O_2Ru$]Br_2: H, 3.27; C, 14.61; N, 22.72; Ru, 20.50. Found: H, 2.82; C, 14.33; N, 22.52; Ru, 20.52. Yield: 45%. $\nu_{C=O} = 1638, 1727$ cm^{-1}.

[(1,3-Me_2Lum)(NH_3)$_4Ru^{II}$]Br_2 was made in an analogous fashion, with the exception that the complex was eluted from the column with 0.35 M HBr. Yield: 55%. HPLC: $k' = 2.73$. Anal. Calcd for [$H_{20}C_8N_8O_2Ru$]Br_2: H, 3.87; C, 18.44; N, 21.50; Ru, 19.39. Found: H, 3.37; C, 18.90; N, 21.51; Ru, 19.99.

[(3-$MePH^+$)(NH_3)$_4Ru^{II}$]Br_3 was similarly prepared, except that the product was eluted from the cation-exchange column with 0.4 N HBr. HPLC: $k' = 1.59$. Using [$Cl(NH_3)_5Ru$]Cl_2 as the starting material produced lower yields. Anal. Calcd for [$H_{20}C_7N_9ORu$]Br_3: H, 3.43; C, 14.32; N, 21.47; Ru, 17.22. Found: H, 2.97; C, 14.23; N, 21.47; Ru, 16.82. Yield: 50–55%. $\nu_{C=O} = 1658, 1717$ cm^{-1}.

[(3,6,7-Me_3PH^+)(NH_3)$_4Ru^{II}$]Br_3 was prepared in the same manner as the 3-methylpterin complex, giving a green amorphous powder. Yield: 45–50%. HPLC: $k' = 2.3$. Anal. Calcd for [$H_{24}C_9N_9ORu$]Br_3: H, 3.93; C, 17.57; N, 20.49; Ru, 16.43. Found: H, 3.75; C, 17.83; N, 19.96; Ru, 16.82. $\nu_{C=O} = 1568, 1778, 1698, 1720$ cm^{-1}.

[(8-MeP)(NH_3)$_4Ru^{II}$]Br_2 was also made by the method described but was eluted from the column with 0.5 M HBr. The yield (20–25%) was lower than for other reactions, perhaps because the ligand exists as 8-$MePH^+$ at the pH of the reaction. HPLC: $k' = 1.18$. Anal. Calcd for [$H_{24}C_9N_9ORu$]Br_3: H, 3.78; C, 16.61; N, 24.90; Ru, 19.97. Found: H, 3.25; C, 16.97; N, 24.15; Ru, 19.63.

Compound Characterization. Elemental analyses were performed by the Stanford Microanalytical Laboratory, Stanford, CA, and Galbraith Laboratories, Knoxville, TN. Magnetic susceptibility measurements were obtained with 20–50-mg samples on a Cahn Model 7500 Faraday balance against a mercury tetrabis(thiocyanato)cobaltate standard.[38] Ruthenium concentrations were measured on an Instrumentation Laboratory Model 551 AA/AE spectrophotometer.[39] A Perkin-Elmer Model 575 spectrophotometer equipped with a digital background corrector and a thermostated sample cell was used for UV-visible spectroscopic studies. Molar absorptivities were measured on solutions obeying Beer's law at an ionic strength of 0.1, unless otherwise specified.

Aqueous pH measurements were made on a Markson Model 90 digital pH/temperature meter equipped with a glass microcombination electrode. pK_a values below pH 1 were determined spectrophotometrically from plots of A vs $(A - A')/[H^+]$, where A' is the absorbance of the fully deprotonated complex and A is the absorbance at a given pH, which yield $-K_a$ as the slope and $A°$, the absorbance of the fully protonated complex, as the intercept. At higher pH, pK_a values were obtained by titrating solutions of the complex over the desired pH range with either a more basic or a more acidic solution containing the complex at the same concentration and ionic strength. Data were fitted to the equation $pK_a = pH + \log[(A - A')/(A° - A)]$. Experiments were performed at 25 °C under an inert atmosphere at $\mu = 1.0$ by using a series of buffers prepared from standardized stock solutions of hydrochloric or perchloric acid and LiCl. For each pK_a, several experiments were performed and isosbestic points were observed in all cases. Corroboration of most of the spectrophotometrically measured pK_a's was obtained from the inflection points of the Pourbaix diagrams.

Fluorescence studies were carried out on a Perkin-Elmer Model 560-10S fluorescence spectrophotometer. Solutions were freshly chromatographed and deaerated with argon just prior to use. A Perkin-Elmer Model 599B grating spectrophotometer was used for all spectra. IR spectra were measured on a Perkin-Elmer Model 1760 FTIR spectrometer in either CsI or KBr pellets. NMR spectra were obtained on a Hitachi Perkin-Elmer Model R-24 NMR spectrometer. Sample concentrations were typically in the range of 10–30 mM.

HPLC studies were carried out on a Varian Model 5000 liquid chromatograph equipped with a Varichrome UV-visible detector and a

Waters μ-Bondapak octadecylsilane (C_{18}) column with a guard column packed with Vydac RP (40-μm glass beads coated with octadecylsilane). The eluant was 0.2 M ammonium propionate, pH 5.5, with a flow rate of 1.5 mL/min.

Electrochemistry. Cyclic voltammetry measurements were made by using a device constructed in this laboratory.[39] A standard all-glass H-cell was used, in which the working and reference compartments were separated by a fine-porosity glass frit. All measurements were made on nitrogen- or argon-purged solutions that were blanketed with the inert gas during the course of the experiment. A three-electrode potentiostat was used, with a Pt-wire auxiliary electrode. The following working electrodes were used: (1) glassy carbon (Bioanalytical Systems), (2) carbon paste (Bioanalytical Systems), (3) platinum disk (Beckman or Corning), and (4) hanging mercury drop (Metrohm). Pretreatment of working electrodes consisted of polishing the glassy-carbon electrode with an aqueous alumina suspension on microcloth (Buehler), with average particle size above 0.05 μm, followed by ultrasonic removal of alumina particles and rinsing with methanol. The platinum electrode was electrochemically pretreated at least five times by placing it in 1 N nitric acid at 1.8 V vs NHE to oxidize impurities for 0.5 min and then switching to 1.2 V for 1 min to remove oxygen formed at the higher potential. The potential was set at 0.05 V and held for 5 min to reduce surface oxides formed in the previous steps.

In aqueous solutions, an aqueous silver/silver chloride microelectrode was used as the reference. In nonaqueous media, either an aqueous Ag/AgCl microelectrode or an Ag/AgCl wire was used. LiCl was used to adjust ionic strength to 0.1 in aqueous solutions, while tetraalkylammonium salts were used in nonaqueous media. A drop of a surfactant (1% Triton X-100) was often used to minimize adsorption effects at the electrode surface in aqueous solution.

After each experiment, an internal standard was added to the working compartment in order to eliminate variables arising from the type of reference electrode, liquid-junction potentials, and reference electrode degradation. In aqueous media, [(NH_3)$_6Ru$]Cl_3 was used as the standard ($E_{1/2} = 57$ mV vs NHE),[40] and in DMF, ferrocene was used ($E_{1/2} = 400$ mV vs NHE).[41] Reversibility was determined on the basis of equal cathodic and anodic peaks, with a separation between these peaks comparable to that observed for the standard, which was usually 60–90 mV. Comparison of peak separations and peak heights to those of an equivalent amount of the standard was used to indicate the number of electrons transferred.[42]

Coulometric studies were carried out in a standard H-cell in DMF that was 0.1 M in tetraethylammonium bromide and ~0.1 M in trifluoromethanesulfonic acid. The sample in the working compartment was continuously stirred with argon. Total charge was determined by using an ECO Instruments Model 551 potentiostat/galvanostat in conjunction with an ECO Instruments Model 731 digital integrator. The electrolysis potential was set at 100 mV cathodic of the $E_{1/2}$ measured by cyclic voltammetry. The electrolysis was allowed to proceed until the current reached a minimum plateau. A blank was then run for the same amount of time, and the result was subtracted from that of the sample to obtain the total coulombs due to the species being analyzed.

Results

Compound Characterization. Since most complexes decomposed over a period of days, even in the process of recrystallization, fresh, quickly precipitated or recently chromatographed samples were necessary for characterization. As the complexes eluted from the ion-exchange column with relatively dilute acid, the deleterious effect of high acid concentrations on the complexes could be minimized by rapid rotary evaporation. Subsequent dissolution and reprecipitation yielded powders that gave good elemental analyses and a single peak by HPLC. Owing to the pK_a's of the coordinated ligands (Table I), the 3-MeP and 3,6,7-Me$_3$P complexes were isolated in their protonated ligand forms.

For the ligands Lum, 1,3-Me$_2$Lum, and 8-MeP, N5 is the only site that is readily sterically available. In the case of 3-MeP and 3,6,7-Me$_3$P, products were obtained with physical properties very similar to those with the more sterically constrained ligands.

(38) Figgis, B. N.; Nyholm, R. S. *J. Chem. Soc.* **1958**, 4190.
(39) Clarke, M. J. *J. Am. Chem. Soc.* **1978**, *100*, 5068.

(40) Lim, H. S.; Barclay, D. J.; Anson, F. C. *Inorg. Chem.* **1972**, *11*, 1460. Yee, E. L.; Cave, R. J.; Guyer, K. L.; Tyma, P. D.; Weaver, M. J. *J. Am. Chem. Soc.* **1979**, *101*, 1131. Matsubara, T.; Ford, P. C. *Inorg. Chem.* **1976**, *15*, 1107.
(41) Gagne, R. R.; Koval, C. A.; Lisensky, G. C. *Inorg. Chem.* **1980**, *19*, 2854.
(42) Goswami, S.; Mukherjee, R.; Chakravorty, A. *Inorg. Chem.* **1983**, *22*, 2825.

Table I. pK_a Values of $[L(NH_3)_4Ru^{II}]$ and Related Free Ligands

| free ligand (L)			Ru–L Complexes		
			Ru(II)	Ru(III)	
L	pK_a	site	$pK_a{}^b$	$pK_a{}^b$	site
LumH^{+a}	−3	N5	−0.9 (s)		N8
Lum	7.96	N3	5.47 (s)	1.89 (e)	N1
			5.76 (e)		
Lum$^-$	12.64	N1	10.65 (s)	7.62 (e)	N3
			10.50 (e)		
3-MeLumH^{+a}	−2.75	N5			
3-MeLumH$^+$	8.00	N1	5.41 (s)		N1
1,3-Me$_2$LumH$^+$	−3	N5	−0.9 (s)		N8
3-MePH$^+$	2.27	N1	2.00 (s)		N8
			2.50 (e)		
3,6,7-Me$_3$PH$^+$	2.60	N8	2.28 (s)		N8
			2.39 (e)		
			2.33 (el)		
8-MePH$^+$	5.42	N1	none detected		
RibH$^+$	0.25	N1	0.7		N1
Rib	10.0	N3	7.4		N3

^{a} Reference 44. ^{b} Key: (s) spectrophotometrically determined; (e) electrochemically determined $(Ru^{II}L/Ru^{III}L)$; (el) electrochemically determined $(Ru^{II}L/Ru^{II}L^-)$.

Infrared spectra of all complexes measured showed substantial perturbations in the carbonyl stretching region. Reactions with 3-methylpterin yielded the same complex when either $[(H_2O)-(NH_3)_5Ru]^{2+}$ or cis-$[(H_2O)_2(NH_3)_4Ru]^{2+}$ was used as the starting material. Elemental analyses revealed the displacement of an ammine from the pentaammine starting material, and the spectra correspond to a series of tetraammineruthenium(II) complexes with similar flavin ligands, whose X-ray structure shows N5–O4 chelation of the metal ion.[43] The complex formed with 1,3-dimethyllumazine exhibited spectroscopic and electrochemical properties nearly identical with those of the lumazine complex, except that it lacked ionizable hydrogens.

Assignments of proton ionization sites in Table I were made by assuming that metal ion coordination at N5–O4 precluded proton binding at these sites and by noting similarities in spectra and pK_a values to those of complexes where alkylation restricted the possible ionization sites. For example, addition of a proton to form the cationic ligand complex of lumazine is taken to be at N8, since the pK_a of −0.9 is similar to that of the complex of 1,3-Me$_2$Lum, which can only protonate at this site. Moreover, the spectra of these two complexes exhibit bands that shift from around 325, 400, and 590 nm in the neutral-ligand species to approximately 340, 415, and 575 nm in the cationic-ligand species.

Spectra. The UV–visible spectral data of these compounds together with those of analogous flavin complexes are listed in Table II. Most complexes showed significant spectral changes with varying pH owing to proton equilibria. Comparison of the fluorescence excitation and emission maxima for the pterin complexes and free ligands (cf. Table III) shows that fluorescence is significantly perturbed by the presence of the metal ion, and only in a few cases is the fluorescence completely quenched. This is in contrast to the case of the analogous flavin complexes, which did not fluoresce, and the molybdopterinate species,[17] which fluoresced only on dissociation of the pterin ligand. As with the free ligands, the fluorescence spectra are pH dependent.[44]

Electrochemistry. The electrochemistry of this class of compounds was investigated by cyclic and square-wave voltammetry in aqueous solution. Anodic scans from the open-circuit voltage revealed all compounds to have a reversible one-electron wave attributable to a Ru(II,III) couple (see Discussion). The redox potential of this wave was pH dependent for each complex that exhibited accessible pK_a's spectrophotometrically. Determined from the pK_a data given in Table I, the pH dependency of the reduction potentials (vs NHE) is given for each complex in Table IV and is shown for the representative E_h vs pH (Pourbaix) plots
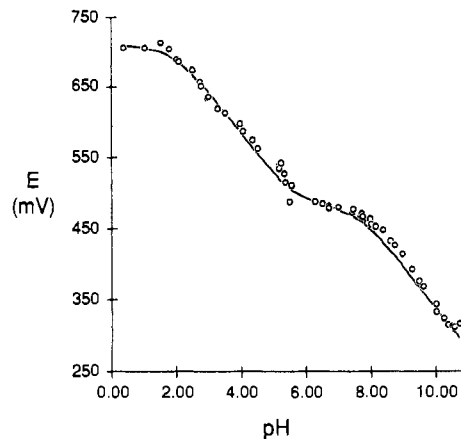
Figure 2. Pourbaix diagram for $[Lum(NH_3)_4Ru^{II,III}]$ in water, $\mu = 0.1$.

E° = 537 ± 2
pKa = 2.33 ± 0.03

E° = −408 ± 2 mV
pKa = 2.39 ± 0.05
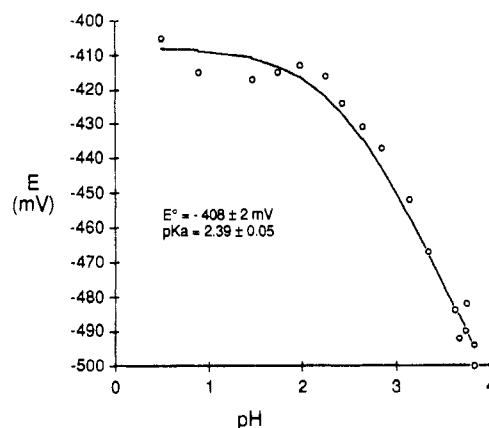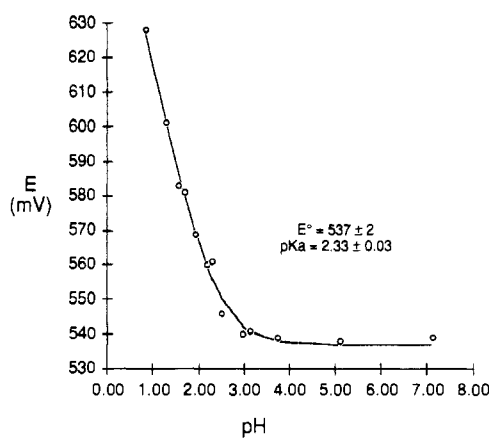
Figure 3. (a) Pourbaix diagram for $[(3,6,7-MeP)(NH_3)_4Ru^{II,III}]$ in water, $\mu = 0.1$. (b) Same as (a) for $[(3,6,7-Me_3P)(NH_3)_4Ru^{II}] + H^+ + e^- \rightarrow [(3,6,7-MePH^\cdot)(NH_3)_4Ru^{II}]$.

for $[Lum(NH_3)_4Ru^{II,III}]$ and $[(3,6,7-Me_3P)(NH_3)_4Ru^{II,III}]$ in Figures 2 and 3a, respectively. Slopes of the Pourbaix plots were 59 mV/pH, which is consistent with a $1e/1H^+$ process.

Scans cathodic of the reference potential generally yielded irreversible wave forms, which are taken to arise from reduction of the pterin ligand. However, on relatively rapid cyclic voltammetric scans (>100 mV/s), the couples for both $[(3,6,7-Me_3P)(NH_3)_4Ru^{II}]$ and $[(3-MeP)(NH_3)_4Ru^{II}]$ appeared somewhat reversible in aqueous solution. The pH dependencies of these couples listed in Table IV are consistent with single-electron reduction of the coordinated pterin. The Pourbaix diagram for ligand reduction of $[(3,6,7-Me_3P)(NH_3)_4Ru^{II}]$ is shown in Figure 3b.

In an attempt to identify the origin of the irreversibility of the ligand reduction process in these complexes, the 1,3-dimethyllumazine complex was electrolyzed potentiostatically for about 20 min at pH 6, until the dark blue color had begun to fade. A cyclic voltammogram of the resulting solution showed that the

(43) Clarke, M. J.; Dowling, M. G.; Garafalo, A. R.; Brennan, T. F. *J. Biol. Chem.* **1980**, *225*, 3472.
(44) Klein, R.; Tatischeff, I. *Photochem. Photobiol.* **1987**, *45*, 55–65.

Table II. UV–Visible Spectral Data for [L(NH$_3$)$_4$Ru^{II}]

ligand	λ_{max}, nm	ϵ, 10^4 M^{-1} cm^{-1}	media	ligand	λ_{max}, nm	ϵ, 10^4 M^{-1} cm^{-1}	media
LumH$^+$	241	1.74	12 N HCl	3,6,7-Me$_3$P	223 (sh)	4.46	pH = 5.92
	250	0.528			243	6.80	acetate
	338	1.61			268	5.53	μ = 0.2
	413	0.289			337	3.23	
	578	0.771			381 (sh)	1.02	
Lum	230	1.99	pH = 2.13		582	2.12	
	322	1.61	glycine/HCl	3-MePH$^+$	245	4.34	pH = 0.7
	400	0.237	μ = 0.1		269	3.34	0.2 N HCl
	594	1.00			338	1.84	μ = 0.2
Lum$^-$	238	2.11	pH = 7.25		383 (sh)	0.446	
	278 (sh)	0.797	phosphate		577	1.87	
	319	1.70	μ = 0.1	3-MeP	256	4.80	pH = 5.85
	360 (sh)	0.327			355	1.54	acetate
	568	1.13			410	0.955	μ = 0.2
Lum^{2-}	213	7.25	pH = 12.4		577	1.77	
	251	4.45	LiOH	8-MeP	259	4.64	pH = 5.88
	333	0.896	μ = 0.1		308 (sh)	0.93	acetate
	391	0.549			361	1.03	μ = 0.2
	550	1.25			415	1.09	
1,3-Me$_2$LumH$^+$	211	5.87	12 N HCl		585	1.70	
	248	4.54		RibH^{+a}	218	1.73	6 M HCl
	290	1.24			259	2.59	
	343	3.04			382	1.04	
	419	0.65			419	1.26	
	574	2.08			604	0.922	
1,3-Me$_2$Lum	238	5.22	pH = 6.34	Rib^a	225	2.14	0.1 M LiCl
	328	3.10	phosphate		267	3.08	pH = 4.6
	400	0.46	μ = 0.1		357	0.613	μ = 0.1
	591	2.21			405	0.768	
3,6,7-Me$_3$PH$^+$	221 (sh)	3.49	pH = 0.7		485	0.690	
	261	6.59	0.2 N HCl		619	0.964	
	276 (sh)	4.16	μ = 0.2	Rib^{-a}	220	2.41	0.1 M LiCl
	334 (sh)	1.41			262	2.43	pH = 12
	365	2.24			350	0.609	μ = 0.1
	423	1.67			375 (sh)	0.685	
	625	2.52			394	0.763	
					485	0.894	
					626	1.00	

^{a} Taken from ref 43.

Table III. Fluorescence Data for Free Pterins and [L(NH$_3$)$_4$Ru^{II}], μ = 0.1

compd	free pterin			[L(NH$_3$)$_4$Ru^{II}]		
	λ_{ex}, nm	λ_{em}, nm^a	medium	λ_{ex}, nm	λ_{em}, nm	medium
Lum	265		pH 4.02	308	389	pH 2.12
	354^a	442	acetate	340^a	446^a	glycine/HCl
Lum$^-$	284		pH 10.13	268		pH 8.65
	292		glycine/LiOH	354^a	446^a	Tris/HCl
	396^a	450				
Lum^{2-}	294 (sh)		pH 12.98	268	422	pH 12.94
	306		LiOH	364	467^a	LiOH
	409^a	472		396 (sh)		
1,3-Me$_2$Lum	256		pH 7.64	256		pH 7.25
	316^a	332	phosphate	288 (sh)		phosphate
				306	358^a	
3-MePH$^+$	286		pH 1.04	no fluorescence		pH 1.21
	340^a	472	HCl			HCl
	360 (sh)					
3-MeP	257		pH 10.14	276		pH 9.13
	285		glycine/LiOH	352^a	440^a	glycine/LiOH
	316					
	379^a	445				
8-MePH$^+$	252 (sh), 293, 340^a	436	pH 1.02	no fluorescence		pH 6.23
			HCl			phosphate
8-MeP	256, 288, 357^a	441	pH 9.56	no fluorescence		
			glycine/LiOH			
3,6,7-Me$_3$PH$^+$	278		pH 0.86	320^a	461^a	pH 1.2
	347		HCl			HCl
	373^a	457				
	392					
3,6,7-Me$_3$P	256		pH 11.53	280		pH 7.62
	292 (sh)		LiOH	328 (sh)		phosphate
	306			355^a	436^a	
	380^a	438				

^{a} Wavelength of maximum intensity.

Table IV. $E°$ Values and pH Dependencies for the Ru(III,II) Couple of Ruthenium Pteridines in Water at 25 °C and $\mu = 1.0^a$

L	$E°(Ru^{III}L \rightarrow Ru^{II}L)$, V	pH dependence[b] of Ru(III,II) couple	$E°(Ru^{II}L \rightarrow Ru^{II}L)$, V
Lum	0.710	$([H^+]^2 + K_{1(III)}[H^+] + K_{1(III)}K_{2(III)})/$ $([H^+]^2 + K_{1(II)}[H^+] + K_{1(II)}K_{2(II)})$	d
1,3-Me$_2$Lum	0.718	no pH dependence for pH >1	-0.752^c
3-MeP	0.635	$K_{1(III)}/(K_{1(II)} + [H^+])$	-0.1^e
8-MeP	0.568	no pH dependence	d
3,6,7-Me$_3$P	0.537	$K_{1(III)}/(K_{1(II)} + [H^+])$	-0.408^f
Rib	0.891	$(K_{1(III)}[H^+] + K_{1(III)}K_{1(III)})/$ $([H^+]^2 + [H^+]K_{1(II)}[H^+] + K_{1(II)}K_{2(II)})$	-0.32

^{a} Conditions: medium, 0.1 M LiCl, WE, glassy carbon; RE, Ag/AgCl; AE, Pt wire; CV scan rate, 125 mV/s; internal reference, $[(NH_3)_6Ru]Cl_3$. ^{b} Roman numeral subscripts refer to ruthenium oxidation state; arabic numbers refer to deprotonation site. Potential at a given pH is calculated from the equation $E_h = E° - 0.0591 \log Q$, where Q is the term given in the table above. ^{c} Cathodic current peak. Complex decomposes at these cathodic potentials, as can be seen by the disappearance of complex with concomitant appearance of a peak at the free-ligand reduction potential. ^{d} Not observable. $^e E_h = E° - 0.0591 \log \{([H^+]^2 + [H^+]K_{1(II)}[H^+] + K_{1(II)}K_{2(II)})/[H^+]^2\}$, $pK_{1(II)} = 1.2$, $pH_{2(II)} = 4.0$. $^f E_h = E° - 0.0591 \log \{(K_{1(II)} + [H^+])/[H^+]\}$, $pK_{1(II)} = 2.3$.

Table V. Reduction Potentials and Number of Electrons Transferred for Free and Ru(II)-Coordinated Pterins in DMF at $[H^+] = 0.1$ M

compd	$E°$, V	$E_{pc} - E_{pa}$, V^a sample	$E_{pc} - E_{pa}$, V^a ref[b]	n (from coulometry)^c
3,6,7-Me$_3$P	-0.38, -0.49	0.075	0.150	2.1 ± 0.2
Ru-3,6,7-Me$_3$P^d	-0.45	0.100	0.100	1.0 ± 0.1

^{a} Ideally for a reversible system $E_{pc} - E_{pa}$ should be 59 mV for a one-electron process and 29.5 mV for a two-electron process. Owing to cell resistance, actual differences are higher. ^{b} Conditions: 0.1 M $(CH_3CH_2)_4Br$, $[F_3CSO_3H] \sim 0.1$ M; WE, glassy carbon; RE, Ag/AgCl; AE, Pt wire; CV scan rate, 125 mV/s; internal reference, ferrocene in DMF. ^{c} Electrolysis performed at a potential 100 mV negative of reduction potential. ^{d} Ru(III) → Ru(II) couple, 0.206 V.

reduction peak of $[1,3-Me_2Lum(NH_3)_4Ru^{II}]$ at -752 mV vs NHE had been replaced by a reduction peak at -720 mV, attributed to free 1,3-dimethyllumazine, with the concomitant appearance of a new redox couple at -58 mV, which is in the range expected for cis-$[(OH_2)(OH)(NH_3)_4Ru^{III}]^+$ (cis-$[(OH_2)_2(NH_3)_4Ru]^{3+}$ $E_{1/2}$ = 0.107 V and cis-$[Cl_2(NH_3)_4Ru]^+$ $E_{1/2}$ = -0.108 V), indicating that the complex undergoes dissociation following reduction.

As already indicated, $[(3,6,7-Me_3P)(NH_3)_4Ru^{II}]$ (and the uncomplexed ligand) exhibited nearly reversible cyclic voltammetric wave forms in acidic aqueous and in nonaqueous solutions on cathodic scans. Comparison of the peak heights and peak separations of the free-pterin reduction couple with those of the same amount of a known reversible couple ($[Ru(NH_3)_6]^{3+,2+}$ in aqueous media and ferrocene in nonaqueous media) indicated that the reduction of the free ligand involved a two-electron reaction. Analogous experiments with the metal complex (see Figures 3b and 4) indicated a one-electron reduction. Controlled-potential coulometry of the 3,6,7-Me$_3$P and its metal complex in DMF (cf. values in Table V) confirmed these determinations.

The cyclic voltammogram of the 8-methylpterin complex exhibited a series of small currents with no well-defined anodic peak, demonstrating the importance of the N8 position in the electron-transfer process and/or the protonation site of the complex. In fact, during the anodic sweep, the peak due to the internal standard was abnormally broad, indicating that the reduction products adsorbed onto the electrode surface, forming an insulating layer. This suggests that the transferred electron resulted in an unstable radical, which may have rapidly polymerized on the electrode surface.

Discussion

Spectra. Close correspondences in their UV–visible spectra indicate a similar coordination site for the various complexes in
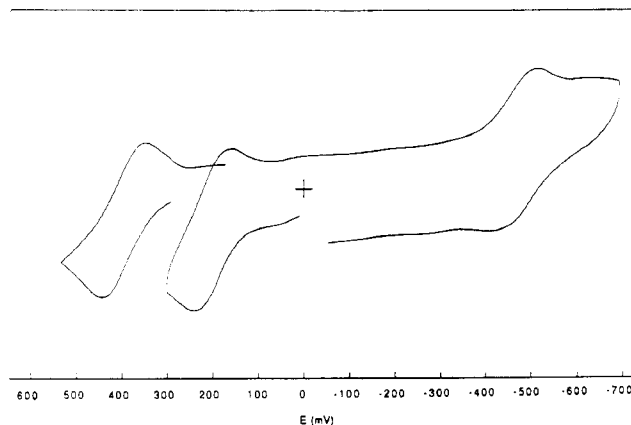

Figure 4. Cyclic voltammetry scan of $[(3,6,7-Me_3P)(NH_3)_4Ru]^{2+}$ in acidic (pH $\sim$ 1.5) 0.1 M tetraethylammonium bromide in DMF using a glassy carbon working electrode and a Ag/AgCl wire reference electrode in an H-cell with the reference electrode on one side and the working and auxiliary electrodes on the other separated by a fine fritt. $[Me_3PRu] = 11.2$ mM, $[Cp_2Fe] = 11.2$ mM. The peak centered at 400 mV is the ferrocene standard.

that all neutral-ligand complexes exhibited an intense metal-to-ligand charge-transfer transition around 600 nm and coordination-induced shifts in the series of $\pi \rightarrow \pi^*$ ligand transitions between 330 and 430 nm. Since ligands were used in which N3 (1,3-Me$_2$Lum, 3-MeP, and 3,6,7-Me$_3$P), N1 (1,3-Me$_2$Lum), and N8 (8-MeP) were blocked by alkylation and the spectra of all complexes are similar to each other and those of an analogous series of flavin complexes in which the coordination site is known,[23,43] chelation is taken to be at N5 and O4. This is supported by the infrared spectra of all complexes, which showed substantial perturbations in the carbonyl stretching region. In the case of lumazine, which was the most easily interpretable, carbonyl stretching bands at 1700 and 1722 cm^{-1} in the free ligand shifted to 1638 and 1727 cm^{-1}, consistent with metal complexation involving significant retrodative bonding at one of the carbonyls. Chelation by N5–O4 is also consistent with the elemental analyses, which indicated the formation of tetraammine complexes, even when the starting material was a pentaammine species.

Comparison of the pK_a's for the lumazine and 3-methyllumazine complexes (cf. Table I) indicates that the pK_a at 5.47 is due to proton loss from the N1 position, while the one at 10.65 is due to deprotonation from N3. The pK_a (-0.9) of $[(1,3-Me_2LumH^+)(NH_3)_4Ru^{II}]$ can be attributed to deprotonation at the N8 site, since all other nitrogen sites are blocked. By analogy, the identical pK_a of $[(LumH^+)(NH_3)_5Ru^{II}]$ is attributed to protonation at N8. In both these complexes the coordinated ligands are substantially more basic than the free molecules. Since free Lum adds H$^+$ at N5, N8 must be more acidic in the free ligand; consequently, the lowering of the pK_a for LumH$^+$ is even more than the 2.1 units indicated by the pK_a values in Table I. Ruthenium(II) complexes with nitrogen-containing aromatic bases feature significant retrodative bonding between the ruthenium d orbitals and π^* orbitals involving nitrogen. This effect increases the basicity of pyrazine by 2 pK_a units[45] and accounts for the substantial increase in the basicity of the pyrazine N8 site in the lumazine complexes.

Free pterin has a pK_a of 7.92 for deprotonation of the N3 position to form the anion and a pK_a of 2.27 for protonation of the N1 position to form the cation. As noted in Table I, 3-MePH$^+$ and 8-MePH$^+$ also ionize from N1. Back-bonding from Ru(II) to the pyrazine ring of the pterins should increase the basicity of the N8 and possibly shift the site of proton addition from N1 to N8. This would account for the 8-methylpterin complex's having no detectable pK_a in the pH range 1–12, since ionization is prevented by the alkyl group on the pyrazine ring and the vacant N1 and N3 sites are not sufficiently basic to protonate in this range.

(45) Ford, P.; Rudd, De F. P.; Gaunder, R.; Taube, H. *J. Am. Chem. Soc.* **1968**, *90*, 1187.

By analogy, proton loss from [(3-MePH$^+$)(NH$_3$)$_4$Ru^{II}] and [(3,6,7-Me$_3$PH$^+$)(NH$_3$)$_4$Ru^{II}] is also taken to be from N8.

In general, the pterin fluorescent excitation bands are shifted to somewhat higher energies, while there is no discernible pattern in the changes in emission frequencies (Table III). This is consistent with an altering of the pterin π molecular orbitals involved in these transitions as a result of Ru(II) retrodative bonding. Protonation of the coordinated pterin ring often quenches the fluorescence, whereas this simply shifts the fluorescence in the free ligands.[44]

Electrochemistry. The pH dependencies for all the Ru(III,II) couples listed in Table IV are consistent with single-electron transfers for this couple. These couples yielded reversible current wave forms by cyclic voltammetry between 540 and 720 mV. Such high reduction potentials are inconsistent with electron-transfer processes involving pterins but are within the expected range for ruthenium ammine centers when coordinated to good π-acceptor ligands.[23,43] Since the pterin and lumazine ligands have only approximately two-thirds of the aromatic ring structure of flavins, it is not surprising that the retrodative bonding is somewhat less and the Ru(III,II) reduction potentials are lower (cf. Table IV). The decrease in the Ru(III,II) $E°$ values in going between the lumazine and pterin complexes results from the change in substituents from an electron-withdrawing oxygen to an electron-donating amine. Similarly, the two additional methyl groups can account for the lower Ru(III,II) potential in the 3,6,7-MeP complex relative to the monomethyl species.

The equilibrium for the tautomerization between the 5,8- and the 7,8-dihydropterin has been reported to favor the 7,8-dihydro derivative, except for C7-substituted pterins.[46] This added stability may explain why [(3,6,7-MeP)(NH$_3$)$_4$Ru^{II}] shows a reversible couple in both DMF and water, while [3-MeP(NH$_3$)$_4$Ru^{II}] exhibits a reversible couple only in DMF, and may also account for the difference in coordinated pterin reduction potentials in both solvents (see Tables IV and V).

The reduction of pterins usually proceeds via a 2e/2H$^+$ pathway to form a 5,8-dihydropterin that tautomerizes to the 7,8-dihydropterin.[47] This can be followed by another 2e/2H$^+$ reduction step to yield the 5,6,7,8-tetrahydropterin (see Figure 1).[46] However, polarographic studies of 8-methylpterin have been interpreted to suggest that blockage of one of the two initial protonation positions in free pterins induces a parallel pathway for the first reduction involving two 1e/1H$^+$ steps[48] with formation of the "5-hydro" semiquinone and the 1,5-dihydropterin that tautomerizes to the 1,7-dihydropterin. Single-electron reduction also appears to be the case for acidic solutions of the complexed pterins reported here, in which coordination at N5–O4 separates the normal two-electron process so that the initial reduction involves a single electron.

The peak heights and peak separations observed by CV for [(3-MeP)(NH$_3$)$_4$Ru]$^{2+}$ or [(3,6,7-Me$_3$P)(NH$_3$)$_4$Ru]$^{2+}$ are consistent with a single-electron reduction for the ligand couple, which is confirmed by the coulometric data in Table V. This shows that while pterins, like the structurally related flavins and purines, have a pronounced tendency to undergo 2e/2H$^+$ redox processes, these can be separated into single-electron steps by coordination of a metal ion in a suitable position. In the case of flavins, this is the site where a significant amount of electron density accumulates in the radical species. Alkylation at N8 and coordination at N5 appear to prevent a reversible, ligand-centered reduction. Since there was evidence for coating the electrode through polymerization, reduction of this complex may proceed in a 1e-reduction fashion with subsequent dimerization of the ligand through C7, as has been observed for 8-MeP at high pH.[49]

Coordination of nitrogen heterocyclic redox of cofactors clearly has a significant effect on whether these molecules undergo one- or two-electron processes.[50] Since pterins are in close proximity to metal ions in a number of electron-transfer enzymes, it is not unreasonable that, in some instances, coordination may occur, so as to modulate the pterin redox couple and/or that of the metal center.

(46) Kwee, S.; Lund, H. *Biochim. Biophys. Acta* **1973**, *297*, 285.
(47) Pfleiderer, W.; Gottlieb, R. In *Biochemical and Clinical Aspects of Pteridines*; Wachter, H., Curtius, H. C., Pfleiderer, W., Eds.; Walter de Gruyter: Hawthorne, NY, 1985; Vol. 4, pp 3–15.

(48) Braun, H.; Pfleiderer, W. *Liebigs Ann. Chem.* **1973**, 1099.
(49) Lung, H. *5th International Symposium on Chemistry and Biology of Pteridines*; Pfleiderer, W., Ed.; Walter de Gruyter: Hawthorne, NY, 1975; pp 645–670.
(50) Clarke, M. J. *Comments Inorg. Chem.* **1984**, *3*, 131–151.